Available online at www.sciencedirect.com
ScienceDirect
Journal of Power Sources 162 (2006) 893–899
JOURNAL OF POWER SOURCES
www.elsevier.com/locate/jpowsour

Performance improvements of alkaline batteries by studying the effects of different kinds of surfactant and different derivatives of benzene on the electrochemical properties of electrolytic zinc

Robab Khayat Ghavami *, Zahra Rafiei

Research & Development Center, Niru Battery MFG. Co., P.O. Box 19575-361, Tehran, I.R. Iran

Received 14 April 2005
Available online 19 August 2005

Abstract

Electrolytic zinc powders were prepared in 12 M KOH, 4 wt.% zinc oxide solutions in the presence of different kinds of surfactant and organic additives using the galvanostatic technique. Then the electrochemical behavior of zinc was investigated using the sweep voltametry technique. Zinc samples electrolyzed in the presence of cationic cetyl trimethyl ammonium bromide (Zn-CTAB), have maximum corrosion rate. Furthermore, scanning electron microscopy revealed the highest surface area. Zinc deposited with anionic surfactants, sodium dodecyl benzene sulfonate (SDBS) and sodium dodecyl sulfate (SDS), have high dendritic and secondary growth. More zinc ions electrolyzed on the cathode electrode in the presence of SDBS compared with SDS. We suppose the Benzene molecule in SDBS changes morphology, thus effects of the benzene molecule is investigated by utilizing several organic compounds during zinc electrodeposition. Naphthalene with 10 pi electrons at two fused rings decreases corrosion rate and needle growth of zinc deposited, compared to benzyl chloride which has 6 pi electrons. Enhanced delocalization of pi electrons by strongly activating group ($–NH_2$) in the aniline molecule increases the corrosion rate and dendrites compared with benzyl chloride, which has the weakly activating group ($–CH_2Cl$). The addition of chloro benzene with inactivating and electrodrawing group (–Cl) creates high surface area without any dendritic growth. The effects of electrolyte additives on the electrochemical capacity of AA-sized alkaline Zn-MnO_2 batteries are verified. The addition of Triton X-100 in anode gel resulted in maximum electrical capacity. Anionic (SDBS and SDS) additives gave higher electrical capacity than cationic (CTAB). Also, the reaction mechanism for zinc electrodeposition in alkaline electrolytes and its dependence upon the presence of organic additives are discussed in detail.

Keywords: Zinc electrodeposition; Alkaline; Surfactants; Derivatives of benzene

1. Introduction

Different morphological and electrochemical properties of electrolytic zinc are obtained under identical experimental conditions except for the surfactant type and its concentrations [1–3]. In 1907 Snowden reported that the addition of small amounts of formaldehyde into the zinc-plating bath reduced the grain size of deposit [4]. Today, a large variety of organic additives is used in zinc electroplating in advanced zinc secondary and primary batteries to obtain a beneficial effect on zinc morphology [5–8]. This includes Quinine derivatives, water-soluble polymers, hetro-cyclic aldehydes and aromatic compounds [9]. Also, surfactants used for different purposes, such as wetting, emulsifying, dispersing, foaming, scouring or lubricity [10]. Different kinds of surface-active agents (anionic, cationic and non-ionic) and fluoro-surfactants are used to modify the zinc electrode [11–14]. The aim of such investigations is to improve appearances and physical–chemical properties of the deposit in areas of corrosion resistance, brightness and grain size. In addition inducing a catalytic process and optimizing the operating parameters of the electroplating bath are of economical interest in industrial processes. Some of the additives in zinc

* Corresponding author. Tel.: +98 21 22547034; fax: +98 21 22582421.
E-mail address: star_khayat@yahoo.com (R.K. Ghavami).

0378-7753/$ – see front matter © 2005 Elsevier B.V. All rights reserved.
doi:10.1016/j.jpowsour.2005.07.010

electrodeposition are specifically adsorbed at rapid growth sites (i.e. dendrites) on the surface of the electrode and restrict further growth at these locations [15,16]. These additives can have an effect on the shape change of the zinc electrode, as well as dendrite growth, cycleability [17], hydrogen evolution reaction, grain size, solubility of zincate product [18–20], etc. Different mechanisms are presented and explained for the interaction of surface-active solutes with the solid substrates and/or ionic species. These are: ion exchange/pairing, acid–base, electronic polarization of π electrons, dispersion forces, hydrophobic/hydrophilic, electrostatic adsorption, or chemisorption bonding [21,22].

Fransaer [23,24] described friction adhesion removal force balances and a modifying of the hydrophobicity of the particles due to adsorption of surfactants. These could affect the electro-osmotic and electro-phoretic forces, which results in a particle co-deposition, especially in an organic/non-organic solution mixture. Kardos [25] gives the relationship between the blocking effects of the adsorbed organic compound and the diffusion of electro-active species to the electrode microprofile. This theory states that the adsorbed organic compounds inhibit the metal deposition on sites, which occupied by the organic molecule. Juhel et al. also proposed that, during cathodic polarization, the surface of the zinc electrode is partially covered by adsorbed surfactant molecules, which block some of active sites of the electrode surface [26]. Perfluoro anionic surfactant (FC-129) induced an increase in hydrogen potential, which may be adsorbed on the surface of the zinc electrode via non-polar groups [27].

However, the reaction mechanism of zinc deposition in alkaline electrolytes and its dependence upon the presence of organic additives is not yet well understood. In battery technology, suppressing gas evolution through the anticorrosion effect of surfactants is of special interest. In this work, the effects of surfactants on the morphology, dendrite growth and electrochemical behavior of the zinc electrode are investigated by CV, SEM and Tafel plots. The reaction mechanism of zinc electrodeposition in alkaline electrolytes and its dependence upon the presence of organic additives are discussed in details. The purpose of this investigation, is to verify the effects of different kinds of surfactant (CTAB, TX100, SDS and SDBS) and several organic additives (e.g. naphthalene, benzyl chloride, aniline and chloro benzene) on the electrochemical properties of zinc and to find a difference between adsorptions positive and negative charge in zinc electrodeposition.

2. Experimental

2.1. Zinc eletrodeposition with different additives and cell tests

In order to produce zinc powder, a porous zinc deposit was prepared from 12 M KOH solution and 4 wt.% ZnO with 12 A dm^{-2} in the presence various additives, all samples electrolyzed in the same time. The name of the different electrolytic zinc powders, with amount of additives used, are presented in Table 1.

Table 1
Name of zinc powders were deposited in electrolyte solution with different amount of additives

Additives ($g\,l^{-1}$)	Name of electrolytic zinc
Sodium dodecyl benzene sulfonate (SDBS)—0.1, anionic surfactant	Zn-SDBS
Sodium dodecyl Sulfate (SDS)—0.1, anionic surfactant	Zn-SDS
Triton X-100—0.1, non-ionic surfactant	Zn-TX100
N-Cetyl *N*,*N*,*N*-trimethyl ammonium bromide (CTAB)—0.1, cationic surfactant	Zn-CTAB
Naphthalin—0.4	Zn-naphthalene
Benzyl chloride—0.4	Zn-benzyl chloride
Aniline—0.4	Zn-aniline

Anionic Zn-SDBS and Zn-SDS samples have higher a density and finer porosity on electrode surface than the cationic (Zn-CTAB) and non-ionic (Zn-TX100) samples, which have low density and compact form on the cathode. During air flow, the Zn-CTAB sample was flammable. Electrolytic zinc deposited with naphthalene and benzyl chloride were spongy in form and Zn-benzyl chloride in air flowing is more flammable. Zinc oxide films easily formed on Zn-CTAB and Zn-benzyl chloride surfaces. Anionic surfactants and aniline decreased the formation of a passive film on the zinc surface.

The effects of these additives on the electrochemical capacity of alkaline AA-sized Zn/MnO_2 batteries were investigated. Zinc anode used to make the batteries were gelled by mixing 30% electrolyte (12 M KOH, 0.1 $g\,l^{-1}$ surfactant), 68% commercial zinc, 1% zinc oxide, 1% C.M.C. and the effects of organic additives on the discharge capacity were tested by the addition of 0.1 g of these materials directly into the anode gel.

2.2. Potentio-dynamic studies

The working electrode was platinum rod of 3 mm diameter. The platinum rod was sealed with Teflon (PTFE), and a larger platinum sheet was used as a counter electrode. An Hg/HgO reference electrode with a Luggin capillary was used in all experiments. Electrolytic zinc powders were deposited with different additives onto the surface of the working electrode, from 12 M KOH solution containing 4 wt.% ZnO at room temperature using the galvanostatic method. The current density for providing a suitable zinc cover with high stability was at a current density of 120 mA cm^{-2}. This current density decreases dendritic growth in zinc electrodeposition [28]. Autolab PGSTAT 30 was used for the potentio-dynamic and galvanostatic

measurements. Tafel plot curves were obtained in a positive going direction over the range −1550 to −1100 mV in 12 M KOH at a constant scan rate of 5 mV s^{-1}. The cell assembly was the same as that in cyclic voltametry. The zinc deposition was kept at −1800 mV versus Hg/HgO for 5 min in 12 M KOH solution, then disconnected, shaken to free-off adsorbed hydrogen bubbles and polarized from −1800 to −500 mV versus Hg/HgO at sweep rates 10 mV^{-1} [29].

3. Results

3.1. Corrosion studies of electrolytic zinc with different additives

Corrosion studies of electrolytic zinc in 12 M KOH at scan rate 5 mV s^{-1} that deposited from 12 M KOH containing 4 wt.% ZnO and various additives at 120 mA cm^{-2} were carried out by linear sweep voltametry technique. The corrosion rate, R_p (polarization resistance) and I_0 (exchange current density) were calculated from the Tafel plots as shown in Table 2a and b. Electrolytic zinc without additive have high corrosion rate as compared with other samples, because of deposition at low current density. The zinc sample, which was prepared in the presence of cationic (Zn-CTAB,) had a higher corrosion rate than non-ionic Zn-TX100, anionic Zn-SDBS or Zn-SDS samples, respectively. Corrosion current decreases from cationic to non-ionic and anionic while corrosion resistance approximately increases. Moreover, the cathodic Tafel slope is greater than the anodic slope. This suggests that the reaction is under cathodic control.

Typical E–log I curves for zinc in 12 M KOH solution containing 4 wt.% ZnO with different kinds of surfactant and organic additives are presented in Fig. 1a and b. Zn-CTAB has a lower cathodic current density for hydrogen evolution and more negative overpotential than the other samples. Also, Zn-SDBS has a minimum passivity current in anodic branches as shown in Fig. 1a. That is to say the surface area decrease from: cationic Zn-CTAB to non-ionic (Zn-TX100) to anionic (Zn-SDS, Zn-SDBS) samples. In addition, corrosion current and corrosion rate in the presence of benzyl chloride increase as compared with Zn-naphthalene and Zn-aniline. Corrosion

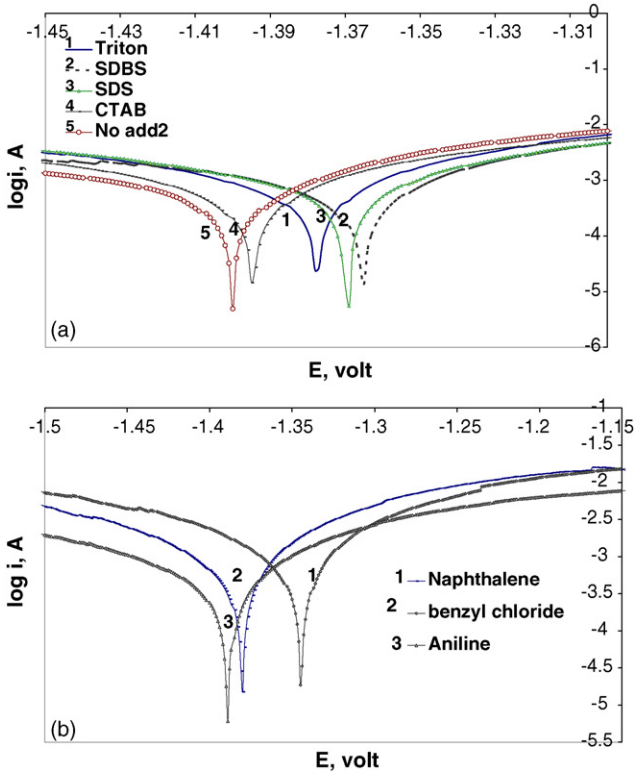

Fig. 1. (a and b) Potentio-dynamic polarization in 12 M KOH for zinc layer on working electrode that deposited from 12 M KOH + 4 wt.% ZnO + different kinds of additive. Potential ranges, −1.1 to −1.55 V. Scan rate, 5 mV s^{-1}; (a) 0.1 g l^{-1} kinds of surfactant, scale of x-axis decrease for better clearness and (b) 0.4 g l^{-1} benzyl chloride and naphthalene.

Table 2
Corrosion studies of zinc in 12 M KOH with different kinds of additives

(a) Different kinds of surfactant

Parameter	Without additive	CTAB 0.1 g l^{-1}	TritonX-100, 0.1 g l^{-1}	SDS, 0.1 g l^{-1}	SDBS, 0.1 g l^{-1}
I_{corr} (A cm^{-2})	0.11	0.157	0.065	0.0381	0.034
b_c (V dec^{-1})	2.2	0.872	0.423	0.227	0.287
b_a (V dec^{-1})	0.24	0.446	0.192	0.115	0.89
R_{corr} (Ω)	21	20	21.9	21.6	22.9
E_{obs} (V)	−1.398	−1.395	−1.384	−1.37	−1.36
Corrosion rate (mm $year^{-1}$)	19	32.9	11.4	6.66	6.07

(b) Organic additives

Parameter	Benzyl chloride 0.4 g l^{-1}	Aniline 0.4 g l^{-1}	Naphthalene 0.4 g l^{-1}
I_{corr} (A cm^{-2})	0.048	0.016	0.024
b_c (V dec^{-1})	0.477	0.377	0.254
b_a (V dec^{-1})	0.223	0.176	0.145
R_{corr} (Ω)	19.4	47	24.5
E_{obs} (V)	−1.344	−1.389	−1.381
Corrosion rate (mm $year^{-1}$)	8.46	6.7	4.1

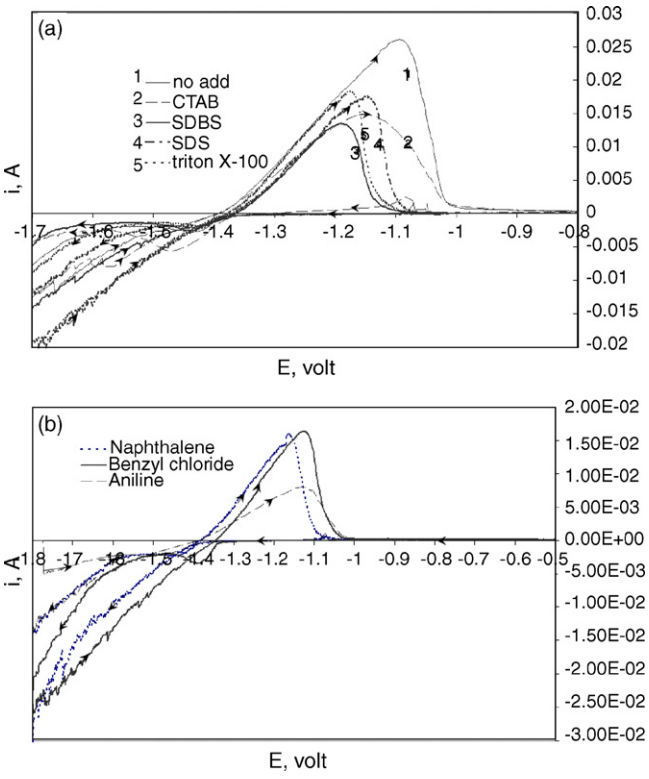

Fig. 2. (a and b) Cyclic voltametry curves recorded for zinc layer in 12 M KOH that deposited from 12 M KOH + 4 wt.% ZnO and different kinds of additive. Potential ranges, −0.5 to −1.8 V. Scan rate, 10 mV s^{-1}; (a) 0.1 g l^{-1} kinds of surfactant and (b) 0.4 g l^{-1} benzyl chloride, naphthalene and aniline.

resistance of Zn-aniline is at a maximum value in line with the results presented in Table 2b. Zn-benzyl chloride has the minimum current passivity as are presented in Fig. 1b. It seems that surface area decreases from Zn-benzyl chloride to Zn-naphthalene and Zn-aniline.

3.2. Cyclic voltametry

Fig. 2a and b gives the cyclic voltametry curves of Zinc electrolytic at scan rate 10 mV s^{-1} in 12 M KOH that deposited at 120 mA cm^{-2} from 12 M KOH containing 4 wt.% ZnO and various additives. During anodic dissolution, significant current peaks appear in −1.1 to −1 V. This corresponds to the precipitation of the zinc oxide film. The anodic peak of zinc dissolution is shifted towards a more positive value in the presence of Zn-CTAB and Zn-benzyl chloride. Zn-CTAB and Zn without additives have a large peak area (Fig. 2a.). The cathodic peak appears around −1.390 V and is related to the reduction of the accumulated $Zn(OH)_2$ and ZnO, formed during the backward cycle in a negative-going direction. These compounds remains on the electrode surface and are not dissolved in the electrolyte [30]. Cathodic peak of Zn-CTAB is noticeable due to the formation of a passive ZnO film on the zinc electrode that has a low electrical resistance and high surface area. However, in Zn-SDBS and Zn-SDS with low current passivity and surface area, decreased ZnO film on the zinc surface which causes cathodic peak, is not observed. Current peak and peak area from anodic dissolution of Zn-benzyl chloride, as compared with Zn-naphthalene and Zn-aniline, increase. That confirmed the reduction of particle adhesion and high electrical resistance of Zn-naphthalene and Zn-aniline as shown in Fig. 3b.

3.3. Deposit morphology

Scanning electron microscopy revealed non-uniform shapes and dendritic growth increase from non-ionic Zn-TX100 to anionic Zn-SDBS, Zn-SDS.

Zn-CTAB has a higher surface area than other samples due to the increase in the adhesion of particles as shown in Fig. 3a. Dendrites and secondary growth in Zn-TX100 are not observed perfectly on the surface (Fig. 3b). By contrast, secondary growth of Zn-SDS is more than Zn-SDBS (Fig. 3c and d). Therefore, the surface area of the zinc in the presence of anionic surfactant decreases through dendrite growth.

Very thin needle-shapes of Zn-benzyl chloride and Zn-naphthalene are shown in Fig. 3e and f. More zinc ions deposited in the presence of Naphthalene in straight lines and in all direction (Fig. 3f) but the adhesion of particles enhances in Zn-benzyl chloride according to Fig. 3e. There is no needle or dendrite growth on surface of Zn-chloro benzene (Fig. 3h) thus surface area is high but Zn-aniline has dendritic growth as shown in Fig. 3g.

3.4. Discharge capacity in commercial cells

Several AA-sized Zn-MnO_2 cells made with different additives in the anode gel were discharged continuously under a constant load of 3.9 Ω. The effects of electrolyte additives on electrical capacity were investigated by the addition of 0.1 g of different surfactants to 12 M KOH electrolyte in 1 liter. Electrochemical capacity is calculated on the basis of active zinc material in the anode gel that was 3.7 g. Fig. 4a presents the discharge curves for different additives. Fig. 4b shows that discharge capacity of zinc anode improves greatly in the presence of non-ionic and anionic [31] surfactants as compared with cationic and without additive. We suggest reduction of electrical capacity follows in this order: non-ionic (TX100), anionic (SDS), anionic (SDBS), cationic (CTAB), without additive. Also, with 0.1 g of benzyl chloride, naphthalene and aniline added to the anode gel directly. The discharge capacity in the presence of benzyl chloride is less than with the other cells.

4. Discussion

In a plating process of zinc, the conditions of electrolysis, such as current density, concentration of ions and temperature in the presence of each additive were constant. Concentration of surfactants is chosen below the C.M.C. point to avoid possible precipitation of surfactants in 12 M KOH. Dodecyl

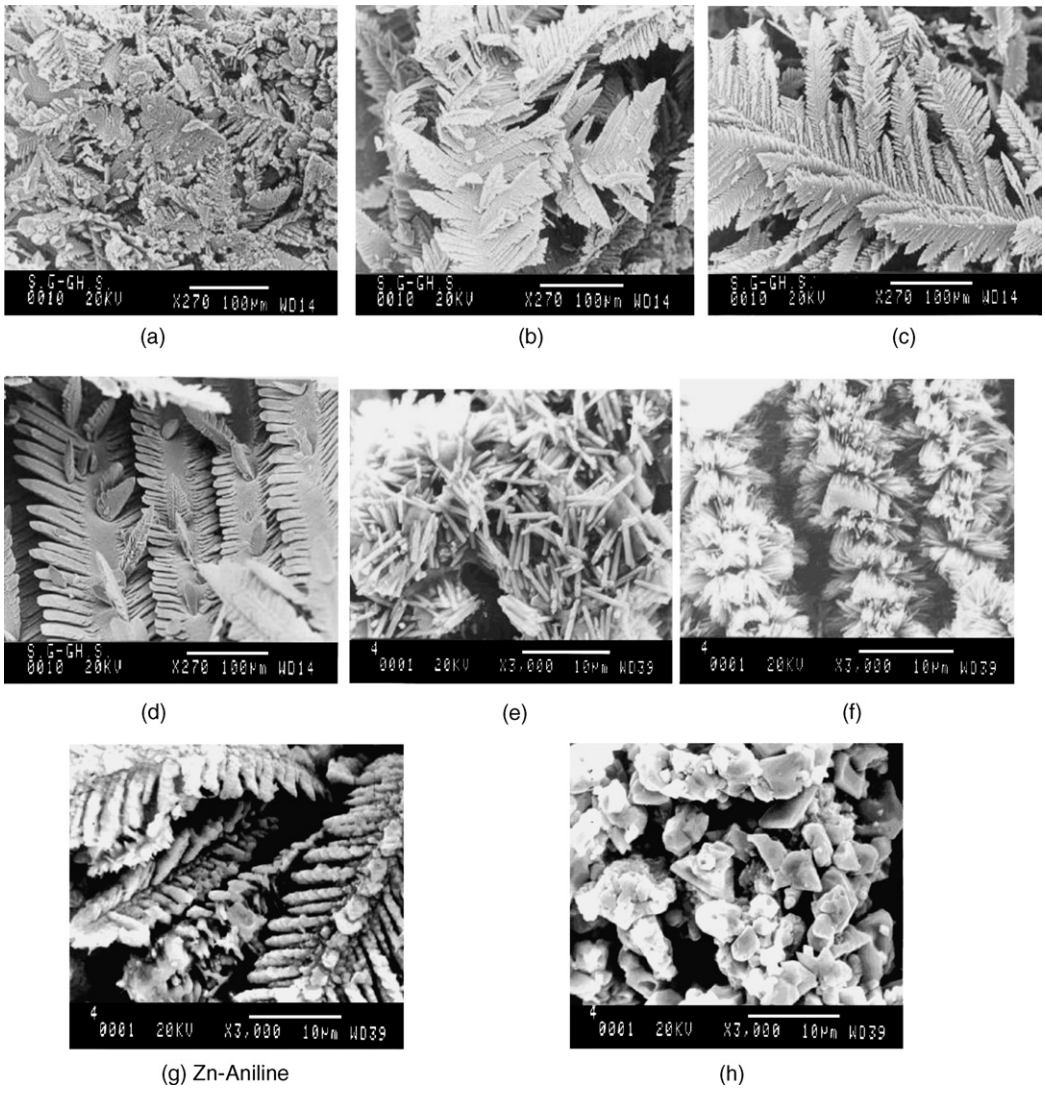

Fig. 3. Electron micrographs of the surface morphology of electrolytic zinc powders deposited in the presences of 0.1 g l^{-1} surfactants and 0.4 g l^{-1} organic additives at 120 mA cm^{-2}. (a) Zn-CTAB, (b) Zn-TX100, (c) Zn-SDS, (d) Zn-SDBS, (e) Zn-benzyl Chloride, (f) Zn-naphthalene, (g) Zn-aniline and (h) Zn-chloro benzene.

benzene sulfonate (SDBS) and dodecyl sulfate (SDS) have similar hydrophilic groups but they create a different morphology. Fig. 3c and d shows that dendrites in Zn-SDBS are wider, but greater secondary growth on Zn-SDS surface is observed. Microstructures of Zn-SDBS show more zinc ions deposited on the same scale at 100 μm as compared with Zn-SDS, however secondary growth is complete. This difference in morphology may be due to the presence of the benzene molecule, which can be more effective than the difference between sulfonate and sulfate groups because benzene has a planer ring of atoms where the electrons, in double bonds, are delocalized over the ring. The pi electrons are thus spread in a molecular orbital above and below the ring [32].

It is important to notice that in the electroplating process, the growth of the crystals occurs by incorporation of an individual metal atom into the crystal lattice. The newly incorporated metal atom is only likely to be stable when it enters the lattice at a site where it interacts with several other atoms already in the lattice. Clearly, the overall phase growth is a sequence of at least three steps. (1) Mass transport in solution (this may be diffusion, convection or migration) of the metal-bearing species to the electrode surface. (2) Electron transfer to form an adatom (one neighbour). (3) Diffusion of the adatom across the surface into a position in the lattice. The structure of the growing layer will be determined largely by the rates of processes (2) and (3) [33].

However, according to the Stern phenomena [32], the solution side of the double layer is divided in two parts: (1) a layer of strongly held counterions, in this case zinc ions adsorbed close to the charged surface on fixed sites (to correct the basic defect of the Gouy-Chapman model) and (2) a diffuse layer of counterions. The electrical potential drops rapidly in the fixed portion (Stern layer) of the double layer and more gradually in the diffuse portion. The fixed counterions

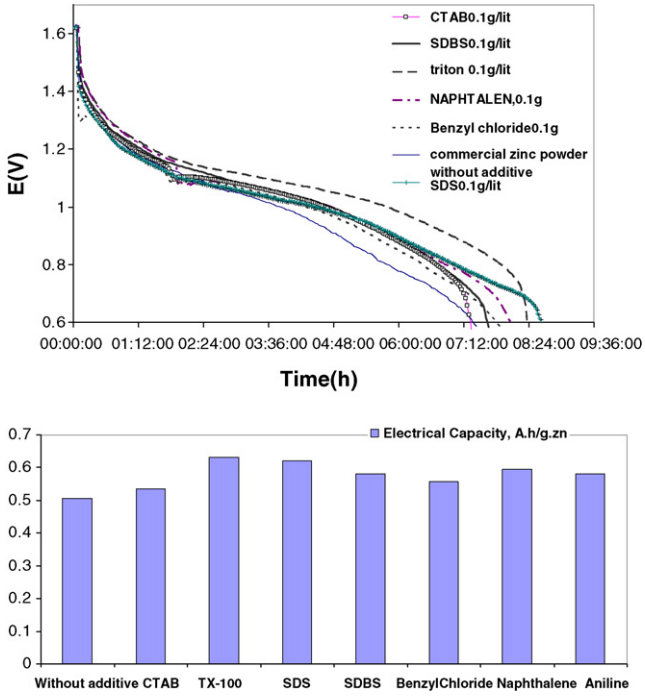

Fig. 4. (a and b) Discharge curves (a) and electrical capacity (b) for a zinc/manganese dioxide cells with different anode gels.

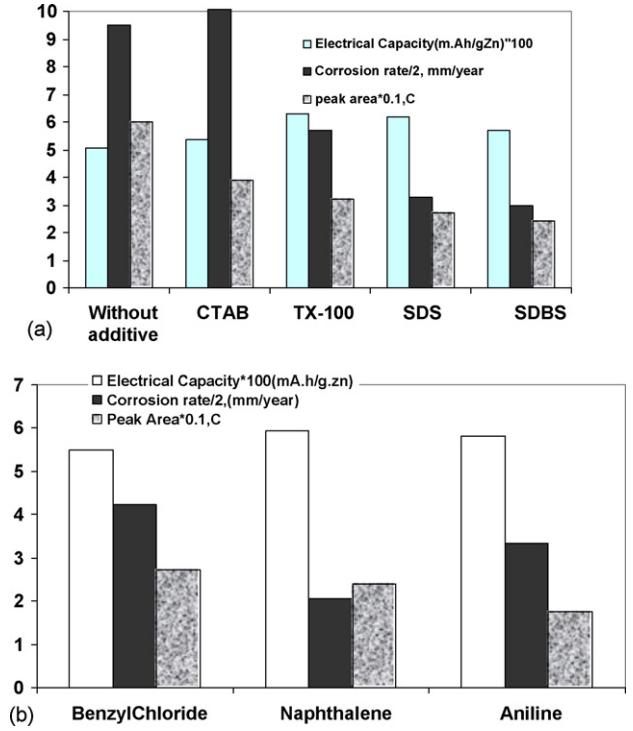

Fig. 5. (a and b) Comparison among of electrical capacity, corrosion rate and peak area for zinc electrodepositions in the presence of different kinds of surfactant (a) and organic additives (b).

in the Stern plane may even change the sign of the potential, resulting from a charged surface, if counter ions have negative charge, such as anionic surfactant. Thus, with the existence of SDBS in the diffuse layer, more zinc ions tend to enter the stern layer because the zeta potential can increase via the delocalization of pi electrons in benzene molecule. It means the potential of the charged surface at the plane of shear between the particle and the surrounding solution [33] in the presence of SDBS increases compared with SDS. The results of this phenomenon are (1) more zinc ions deposited in the same scale which have outward growth because adatoms does not have enough time to diffuse into the crystal lattice (2) dendrites in the presence of SDBS are wider. By contrast, secondary growth on dendrites in the presence of SDS is complete, which is possible to be created from the volume of micelles or the characteristic property of surfactant. This property shows that they spontaneously aggregate in water and form well-defined structures, such as spherical, cylinders, bilayers, etc. [34].

There are different ideas about crystal growth in the presence of cationic surfactant CTAB [35–37]. If CTAB were in the diffusion layer, migration of zinc ions in the Stern plane is difficult because they have similar charge in sign. So zinc ions hardly migrate towards cathode. The results are (1) zinc ions deposited on the same scale at 100 μm should be decreased compared with anionic surfactant as shown in Fig. 1. (2) Adhesion of particles increases as adatom has enough time for diffusing and finding a favoured position in crystal lattice. (3) Corrosion rate increases due to more adhesion of particles and also the surface area is higher. Our observations in zinc deposition, which were obtained by Tafel plots, cyclic voltametry and scanning electron microscopy are explained by this phenomena. The effect of additives on some parameters, such as electrical capacity, corrosion rate and peak area are compared in Fig. 5a and b. Peak area and peak width were suitable parameters from analysis of cyclic voltametry and these the parameters rise with the increase in anodic dissolution. It can be seen from Fig. 5a and b. corrosion rate and peak area in Zn-CTAB increases with the reduction of discharge capacity, while it is the opposite in anionic Zn-SDS and Zn-SDBS samples according to Fig. 5a. We suggest that the positive head group of cationic surfactants promotes the cathodic current distribution, which may prevent dendritic growth. On the contrary, the negative group of anionic surfactants inhibits the diffusion of adatoms across the surface into the proper sites of the growing crystal lattice causing increased dendritic growth.

In order to obtain the effects of delocalization of the electrons in the pi orbital of the benzene molecule and its derivatives in the change of morphology and corrosion rates, we examined three Merk materials, such as benzyl chloride, Naphthalene and Aniline where their solubility in water were reported 0.46, 0.3 and 36 g l^{-1} at 20 °C. There is an important difference between benzyl chloride and naphthalene molecules, because naphthalene has 10 pi electrons which speared in below and above on two fused rings, while benzyl chloride has 6 pi electrons. Usage of these materials in zinc electrodeposition shows: (1) corrosion rate in the pres-

ence of benzyl chloride increases. (2) Naphthalene molecule increases needle and volume growth in all directions on straight line of zinc deposition compared with Zn-benzyl chloride on the same scale at 10 μm (Fig. 3e and f). Therefore, the diminution of pi electrons restricts the needle growth of zinc in the presence of benzyl chloride. Because the existence of the Naphthalene molecule with 10 pi electrons in diffuse layer helps many zinc ions to migrate from bulk solution to the electrode surface for deposition, although the surface diffusion is slow compared with electron transfer which creates coral-shapes. In addition, the kind of substitution groups on the benzene molecule is very important because nearly all groups fall into one of two classes: activating groups, such as $–NH_2$, –OH groups and deactivating groups, such as –Cl, $–NO_2$, $–SO_3H$ [38]. Also, we expect that aniline with strongly activating groups ($–NH_2$) on benzene compared to benzyl chloride which have weakly activating group ($–CH_2Cl$) to decrease corrosion rate and an increase in dendritic growth. Micrograph of Zn-benzyl chloride hasnot shown any dendrite growth but the presence of aniline has shown many zinc ions deposited on the surface with dendritic growth (Fig. 3g). To complete the work, choloro benzene with inactivating and electrodrawing group (–Cl) showed that –Cl substitution decreases the delocalization of pi-electron in pi orbital. A micrograph of Zn-chloro benzene did not reveal any needle or dendrite growth, thus this sample has the highest surface area. It can be seen from Fig. 5b the decreasing of delocalization of pi electrons by the inactivating group in benzyl chloride increases corrosion rate and peak area, while decreasing electrical capacity as compared with the other samples. That is to say that some organic compounds affect local current densities adjacent to the electrode and cause electron transfer to occurs faster than surface diffusion and further nuclei must form. The layer will be less ordered and depend upon: molecular structure, number of atoms, non-bonding electron, pi electron and especially the presence of the benzene molecule and derivates.

Acknowledgments

Our research programs in this domain are supported by the Niru Mfg. Company. We appreciate, Mr. S.M. Tabatabaei, the manager of research and development center and also Mr. A. Shahriyari, the manager of Niru Mfg. Company.

References

[1] A.R. Despic, D. Jovanovic, T. Rakic, Electrochim. Acta 21 (1976) 63.
[2] T.P. Dirksd, J. Electrochem. Soc. 126 (1979) 541.
[3] T. Keily, T.J. Sinclair, J. Power Sources 6 (1981) 47.
[4] R.C. Snowden, J. Phys. Chem. 11 (1907) 369.
[5] D.J. Mackinnon, J.M. Brannen, J. Appl. Electrochem. 12 (1982) 21.
[6] J. Bressan, R. Wiart, J. Appl. Electrochem. 9 (1979) 615.
[7] D.T. Chin, S. Ventakesh, J. Electrochem. Soc. 128 (1981) 1439.
[8] L. Binder, K. kordesch, Electrochim. Acta 31 (1986) 255.
[9] K. Boto. Department of Defence, Materials Resear labratories, A Scot-Vale, Vic. 3032 (Australia).
[10] G.D. Parfitt, C.H. Rochester, Adsorption from Solution at the Solid Liquid Interface, Academic Press, New York, 1983, p. 105.
[11] R. Shivkumar, G.P. Kalaigan, T. Vasudevan, J. Power Sources 75 (1998) 90–100.
[12] J. Kan, H. Xue, S. Mu, J. Power Sources 74 (1998) 113–116.
[13] C.D. Iacovangelico, F.G. Will, J. Electrochem. Soc. 132 (1985) 851.
[14] Meidensha Electric Mfg. Co. Ltd., Jpn. Patent, 82,119,466 (1982).
[15] J.W. Diggle, A. Damjanovic, J. Electrochem. Soc. 117 (1970) 65.
[16] J.W. Diggle, A. Damjanovic, J. Electrochem. Soc. 119. (1972).
[17] L. Binder, W. Odar, K. Kordesh, J. Power Sources 6 (1981) 271–289.
[18] R.E.F. Einerhand, W. Visscher, J.J.M. de Goeij, E. Barendrecht, J. Electrochem. Soc. 138 (1991) 1.
[19] R.E.F. Einerhand, Ph.D. Thesis, Eindhoven University of Technology, Netherlands, 1989.
[20] A.L. Rudd, C.B. Breslin, Electrochim. Acta 45 (2000) 1571–1579.
[21] D.L. Riggs, in: C.C. Nathan (Ed.), Corrosion Inhibitors, National Association of Corrosion Engineers, Houston, TX, USA, 1973, p. 12.
[22] M.J. Rosen, Surfactant and Interfacial Phenomena, second ed., John Wiley & Sons, New York, 1989, p. 39.
[23] J. Francaer, J.P. Celisand, J.R. Roos, J. Electrochem. Soc. 159 (1992) 413.
[24] J. Francaer, Ph.D. Thesis, Catholic University of Leuven, 1994.
[25] O. Kardos, Plating, 61, 129, 229, 316 (1974).
[26] C. Juhel, B. Beden, C. Lamy, J.M. Legger, Electrochim. Acta 35 (1990) 479.
[27] J.L. Zhu, Y.H. Zhou, C.Q. Gao, J. Power Sources 72 (1998) 231–235.
[28] C.C. Yang, S.J. lin, J. Power Sources 112 (2002) 174–183.
[29] S. Barnatt, J. Electrochem. Soc. 39 (1952) 549.
[30] K. Bass, P.J. Mitchell, G.D. Wilcox, J. Power Sources 24 (1988) 21–29.
[31] H. Yang, Y. Cao, X. Ai, L. Xiao, J. Power Sources 128 (2004) 97–101.
[32] J. Daintith, Aromatic Compound, The Facts On File Dictionary of Chemistry, New York NY, Facts On File Inc., 1999, www.factsonfile.com.
[33] D. Pletcher, F.C. Walsh, Industrial Electrochemistry, second ed., Chapman and Hall, 1991, p. 394.
[34] H. Ju. Butt, K. Graf, M. Kappl, Physics and Chemistry of Interfaces, Wiley–VCH Verlag & Co. KGaA, 2003, p. 247.
[35] K. Helle, Report AKZO Research, Arnhem, 1993.
[36] P.K.N. Bartlett, Industrial Traning Report AKZO, Arnhem, 1980, pp. 10–39.
[37] K.S Helle, Proceedings of the Fourth International Conference on Organic Coating Science and Technology, Athens, 1978, p. 264.
[38] Morrison and Boyd, Organic Chemistry, fifth ed., www.ciencemadness.org.